The Observed Hemispheric Symmetry in Reflected Shortwave Irradiance

AIKO VOIGT, BJORN STEVENS, JÜRGEN BADER,* AND THORSTEN MAURITSEN

Max Planck Institute for Meteorology, Hamburg, Germany

(Manuscript received 6 March 2012, in final form 3 July 2012)

ABSTRACT

While the concentration of landmasses and atmospheric aerosols on the Northern Hemisphere suggests that the Northern Hemisphere is brighter than the Southern Hemisphere, satellite measurements of top-of-atmosphere irradiances found that both hemispheres reflect nearly the same amount of shortwave irradiance. Here, the authors document that the most precise and accurate observation, the energy balanced and filled dataset of the Clouds and the Earth's Radiant Energy System covering the period 2000–10, measures an absolute hemispheric difference in reflected shortwave irradiance of 0.1 W m^{-2}. In contrast, the longwave irradiance of the two hemispheres differs by more than 1 W m^{-2}, indicating that the observed climate system exhibits hemispheric symmetry in reflected shortwave irradiance but not in longwave irradiance. The authors devise a variety of methods to estimate the spatial degrees of freedom of the time-mean reflected shortwave irradiance. These are used to show that the hemispheric symmetry in reflected shortwave irradiance is a nontrivial property of the Earth system in the sense that most partitionings of Earth into two random halves do not exhibit hemispheric symmetry in reflected shortwave irradiance. Climate models generally do not reproduce the observed hemispheric symmetry, which the authors interpret as further evidence that the symmetry is nontrivial. While the authors cannot rule out that the observed hemispheric symmetry in reflected shortwave irradiance is accidental, their results motivate a search for mechanisms that minimize hemispheric differences in reflected shortwave irradiance and planetary albedo.

1. Introduction

Earth is subject to boundary conditions that do not fulfill hemispheric symmetry. In particular, most landmasses and the major part of the atmospheric aerosol loading (Geogdzhayev et al. 2005; Kishcha et al. 2009) are located north of the equator. This suggests that the Northern Hemisphere should reflect more shortwave irradiance than the Southern Hemisphere but, when Vonder Haar and Suomi (1971) presented satellite-based estimates of top-of-atmosphere (TOA) irradiance for the period 1962–66, they reported that the Northern and Southern Hemispheres in the annual mean nearly reflect the same amount of shortwave irradiance. The hemispheric symmetry in reflected shortwave irradiance was again noted by Ramanathan (1987), who also pointed out the importance of clouds for the planetary albedo as they compensate the hemispheric difference in clear-sky reflected shortwave irradiance that results from the asymmetric distribution of continents and aerosols.

Subsequent observational TOA irradiance datasets also reported small hemispheric differences in reflected shortwave irradiance, though this information was often buried in large tables. Earth Radiation Budget Experiment (ERBE) data from 1985 to 1989 showed a hemispheric difference of 0.2 W m^{-2} (Hatzianastassiou et al. 2004a), while in the 1985–88 ISCCP data the hemispheric difference was 0.9 W m^{-2} (Zhang and Rossow 1997). Feeding a radiative transfer model with a blend of observational and reanalysis data from 1984 to 1993, Hatzianastassiou et al. (2004b) found a hemispheric difference of 0.1 W m^{-2}.

Today, the Clouds and the Earth's Radiant Energy System (CERES; Wielicki et al. 1996) measures TOA irradiances with previously unachieved precision and accuracy. Among other products, CERES has provided the three editions 1A, 2.5A, and 2.6r for energy balanced and filled (EBAF) data of monthly-mean all-sky and clear-sky irradiances on a 1° × 1° grid since March 2000 (Loeb et al. 2009). In all three CERES-EBAF editions, the time-mean hemispheric difference in reflected shortwave

* Additional affiliation: Bjerknes Centre for Climate Research, Uni Research, Bergen, Norway.

Corresponding author address: Aiko Voigt, Max Planck Institute for Meteorology, Bundesstr. 53, 20146 Hamburg, Germany.
E-mail: aiko.voigt@zmaw.de

DOI: 10.1175/JCLI-D-12-00132.1

TABLE 1. Hemispheric averages of time-mean TOA irradiances as measured by CERES-EBAF (W m^{-2}).

	Northern Hemisphere	Southern Hemisphere	Diff
Edition 1A (March 2000–February 2005)			
Incident shortwave	339.9	339.9	0.0
Reflected shortwave (all sky)	99.5	99.6	−0.1
Reflected shortwave (clear sky)	55.5	49.5	6.0
Longwave (all sky)	240.2	239.0	1.2
Longwave (clear sky)	271.0	267.9	3.1
Edition 2.5A (March 2000–February 2010)			
Incident shortwave	340.0	340.0	0.0
Reflected shortwave (all sky)	99.4	99.5	−0.1
Reflected shortwave (clear sky)	55.5	49.3	6.2
Longwave (all sky)	240.3	238.9	1.4
Longwave (clear sky)	267.2	264.9	2.3
Edition 2.6r (March 2000–February 2010)			
Incident shortwave	340.1	340.1	0.0
Reflected shortwave (all sky)	99.7	99.6	0.1
Reflected shortwave (clear sky)	55.5	49.3	6.2
Longwave (all sky)	240.4	239.1	1.3
Longwave (clear sky)	267.2	264.9	2.3

irradiance does not exceed 0.1 W m^{-2}, which is only 0.1% of the global-mean reflected shortwave irradiance (see Table 1). In conjunction with the symmetric incident shortwave irradiance,[1] this implies hemispheric symmetry in planetary albedo. The hemispheric difference in reflected shortwave irradiance stays below 1 W m^{-2} during individual 12-month periods (Fig. 1, left). In clear-sky conditions, the Northern Hemisphere reflects 6 W m^{-2} more than the Southern Hemisphere, consistent with the fact that most landmasses and the major part of the atmospheric aerosol loading are located north of the equator. Longwave irradiance differs between the hemispheres by 1.2–1.4 W m^{-2}: that is, by 0.5% of the global-mean longwave irradiance. Moreover, the hemispheric difference in all-sky longwave irradiance during all 12-month periods is larger than 0.6 W m^{-2} (Fig. 1, right). The hemispheric symmetry in reflected shortwave irradiance, but asymmetry in longwave irradiance implies northward energy transport across the equator.

The agreement between diverse TOA irradiance datasets indicates that the hemispheric symmetry in reflected shortwave irradiance is a robust feature of the observed climate system. In particular, the hemispheric symmetry is seen in all three editions of CERES-EBAF despite the fact that the editions differ in their CERES input data and use of auxiliary data (see the editions' data quality summaries provided by the CERES Science Team). For example, editions 1A and 2.5A are based on data from the *Terra* satellite alone and explicitly rely on data from geostationary satellites to fill in the diurnal cycle; edition 2.6r uses data from both the *Terra* and *Aqua* satellites and uses scene-dependent diurnal correction factors for shortwave irradiances to remove geostationary satellite artifacts present in the earlier editions. As a consequence, the time-mean reflected shortwave irradiance of editions 2.5A and 2.6r differ by up to 10 W m^{-2} regionally (not shown), but these regional observational uncertainties apparently do not affect the hemispheric difference.

The main goal of this paper is to test whether the observed hemispheric symmetry in reflected shortwave irradiance is a trivial property of the Earth system in the sense that any reasonable partitioning of Earth into two random halves shows hemispheric symmetry in reflected shortwave irradiance. The test requires us to estimate the spatial degrees of freedom of the reflected shortwave irradiance, a task for which we devise a variety of methods. The test is important because, only if the hemispheric symmetry in reflected shortwave irradiance is not a trivial property of the Earth system, future studies should investigate if the hemispheric symmetry is a result of mechanisms that act such as to minimize the hemispheric difference in reflected shortwave irradiance.

2. Is the observed hemispheric symmetry in reflected shortwave irradiance a trivial property of the Earth system?

The observed hemispheric symmetry in reflected shortwave irradiance is a surprising property of the Earth system, in particular given the 6 W m^{-2} hemispheric

[1] Despite nonzero obliquity and eccentricity, the two hemispheres receive the same annual-mean incident shortwave irradiance because Earth moves faster when it is closer to the sun (Kepler's second law). The hemispheric symmetry in annual-mean incident shortwave irradiance can be demonstrated by numerically solving for Earth's movement around the sun following the equations given in, for example, sections 7.3 and 7.5 of Pierrehumbert (2010).

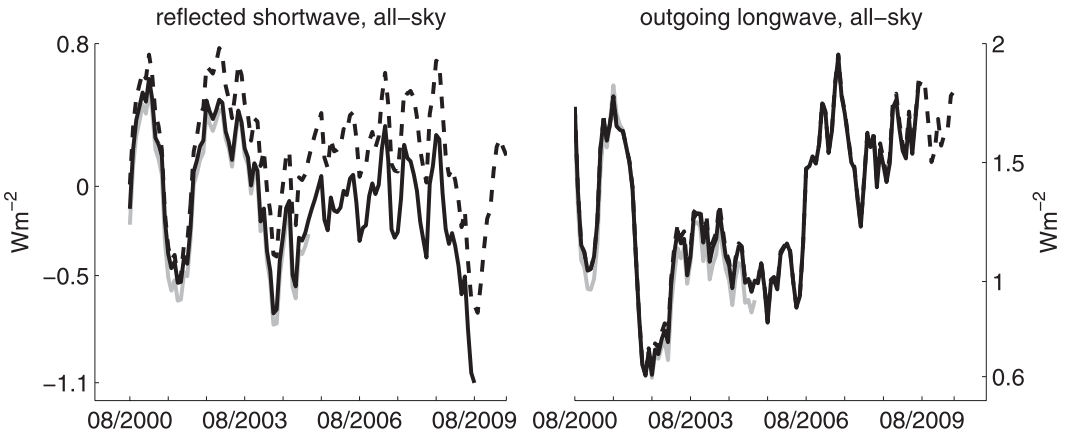

FIG. 1. Twelve-month running mean of hemispheric difference (Northern Hemisphere minus Southern Hemisphere) as measured by CERES-EBAF (solid gray: edition 1A; solid black: edition 2.5A; dashed black: edition 2.6r) for all-sky (left) reflected shortwave and (right) longwave irradiance.

difference in clear-sky reflected shortwave irradiance caused by the asymmetric distribution of continents and aerosols between the hemispheres. Nevertheless, one might suspect that the hemispheric symmetry in reflected shortwave irradiance is a trivial property of the Earth system in the sense that, for any partitioning of Earth into two random halves, the difference of these random halves' reflected shortwave irradiance is nearly zero. For example, in the limit of zero spatial variability (i.e., spatially uniform reflected shortwave irradiance), the hemispheric symmetry would be a trivial property of the Earth system. Similarly, if spatial variability was small and the reflected shortwave irradiance had many spatial degrees of freedom, randomly choosing half of Earth's area might be sufficient to closely sample the global-mean value of reflected shortwave irradiance. In this case, the hemispheric symmetry would also be trivial. Indeed, the time-mean reflected shortwave irradiance shows a comparably low spatial variability (spatial standard deviation of 18.7 W m^{-2} compared to 29.8 W m^{-2} for longwave irradiance: values for CERES-EBAF edition 2.5A) that results from the compensation of the poleward decrease of incident shortwave irradiance by the poleward increase in planetary albedo (Fig. 2, left and middle).

To test if the hemispheric symmetry in reflected shortwave irradiance is a trivial property, we partition Earth into pairs of nonoverlapping random halves. This is done by first dividing Earth into longitude–latitude boxes of size ($\Delta\lambda$, $\Delta\phi$). A pair of random halves is then

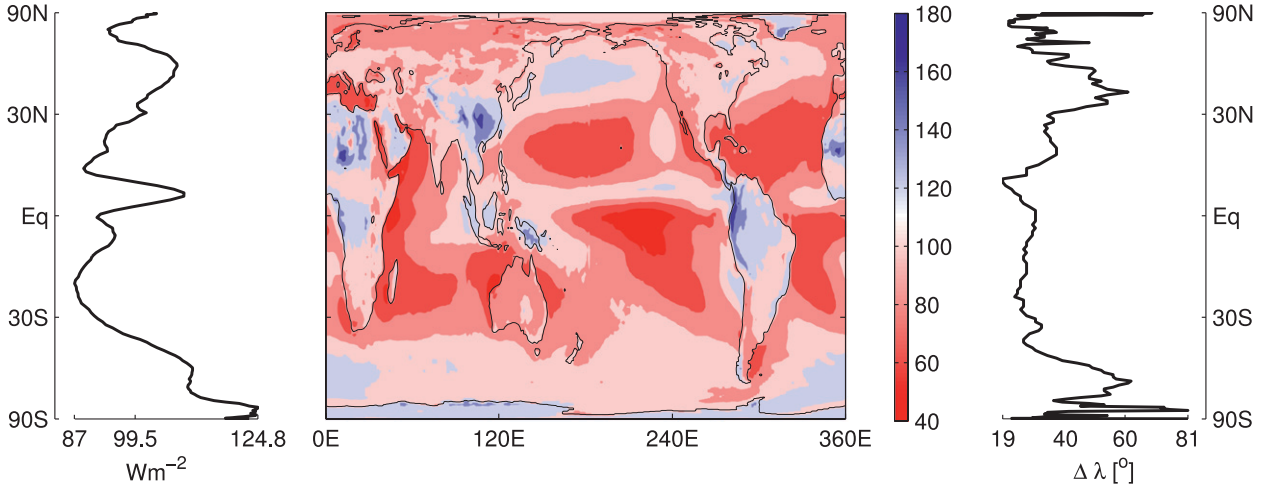

FIG. 2. Time-mean reflected shortwave irradiance from CERES-EBAF edition 2.5A (March 2000–February 2010): (left) zonal average; (middle) longitude–latitude plot; and (right) for each latitude, estimate of $\Delta\lambda$ based on the 95% significance level of the autocorrelation function in the zonal direction. CERES-EBAF edition 2.5A is used.

generated by randomly assigning these boxes to either one of the two random halves while demanding that each random half covers 50% of Earth's area. In most cases, this requires us to split one box between the two random halves. The set of longitude–latitude boxes contributing to any particular half is allowed to be noncontiguous. By this definition, the Northern and Southern Hemispheres are a particular partitioning of Earth for which all boxes of the first random half are located north of the equator. Using time-mean data from CERES-EBAF edition 2.5A, we then calculate how much the reflected shortwave irradiance differs between the two random halves of a given pair; this difference is measured by δR in W m^{-2}. We use time-mean data because the interannual variation of the reflected shortwave irradiance is small for most grid boxes (Kato 2009). By drawing 10^6 pairs of random halves, we determine the percentage P of symmetric pairs of random halves with $\delta R < D$, where D is yet to be determined. If P were close to 100% (i.e., if almost every pair of random halves showed a small hemispheric difference), we would conclude that the hemispheric symmetry of the reflected shortwave irradiance is a trivial property of the Earth system.

The lower the spatial variability and the more spatial degrees of freedom the reflected shortwave irradiance has, the more likely it is to sample the global-mean reflected shortwave irradiance by a random half of Earth. Our test hence essentially is a competition between the spatial variability of the reflected shortwave irradiance and its spatial degrees of freedom. A formal description of this point is given in section 3. While we know the spatial variability from the CERES-EBAF observations, we need to estimate the spatial degrees of freedom. In particular, this is necessary because the reflected shortwave irradiance is organized in spatial structures that each cover several 1° × 1° boxes of the native CERES-EBAF grid (Fig. 2, middle). This implies that we should not draw our random halves on the native CERES-EBAF 1° × 1° grid. Instead, we need to choose the size ($\Delta\lambda$, $\Delta\phi$) of the longitude–latitude boxes such that the value of the reflected shortwave irradiance in a given box can be considered to be independent from the values in adjacent grid boxes. This task is equivalent to estimating the spatial degrees of freedom of the reflected shortwave irradiance, $N = (360°/\Delta\lambda)(180°/\Delta\phi)$.

We first estimate the spatial degrees of freedom in the zonal direction. For each latitude, we calculate the autocorrelation function in the zonal direction and define $\Delta\lambda$ as the lag for which the autocorrelation function first drops below the 95% significance level (Fig. 2, right). The value of $\Delta\lambda$ varies with latitude, with higher values where the reflected shortwave irradiance has a nearly zonally symmetric structure (e.g., in most parts of the Southern Ocean) and low values for regions with larger zonal variations (e.g., around 10°N). The value of $\Delta\lambda$ does not drop below 19° at any latitude, and its area-weighted mean is 36°. This suggests $\Delta\lambda = 36°$ for the zonal width of the longitude–latitude boxes, which is equivalent to 10 spatial degrees of freedom in the zonal direction. We note that if we assumed that the zonal structure of the reflected shortwave irradiance can be described by a first-order autoregressive model, we would have arrived at a similar estimate $\Delta\lambda = [(1 + \rho)/(1 - \rho)] = 40°$ (Fortin and Dale 2005), with $\rho = 0.952$ being the area-weighted mean autocorrelation function at lag 1.

To estimate the spatial degrees of freedom in the meridional direction, we use zonal-mean time-mean reflected shortwave irradiance and follow three different approaches (Fig. 3). First, we calculate the standard deviation on the native CERES-EBAF 1° latitude grid

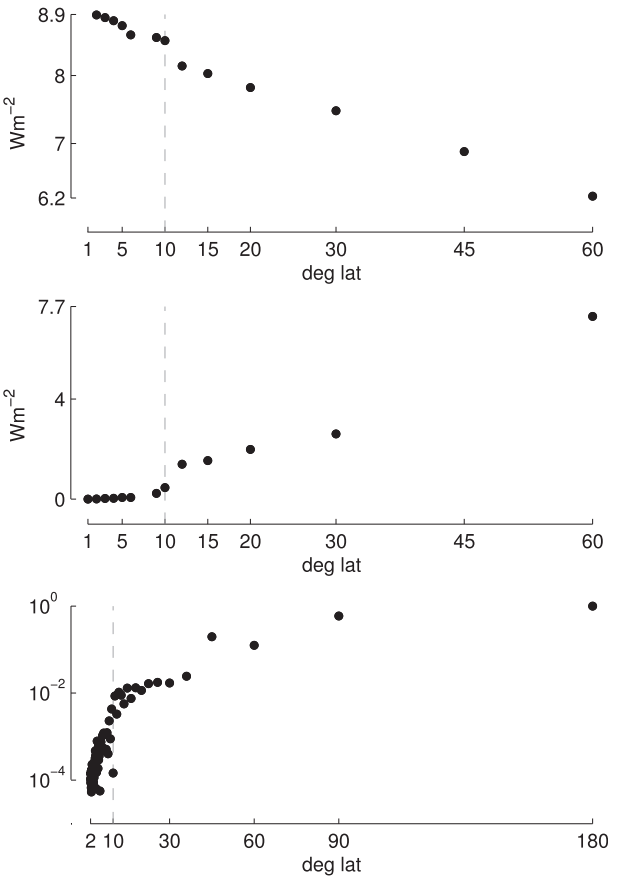

FIG. 3. Estimation of $\Delta\phi$ using zonal-mean, time-mean reflected shortwave irradiance. (top) Standard deviation on native 1°-latitude CERES-EBAF grid as well as various coarser grids with meridional grid spacing given on the x axis. (middle) Maximum deviation of global-mean reflected shortwave irradiance from that of subsamples that only take into account every nth latitude circle. (bottom) Power spectrum as a function of meridional wavelength. CERES-EBAF edition 2.5A is used.

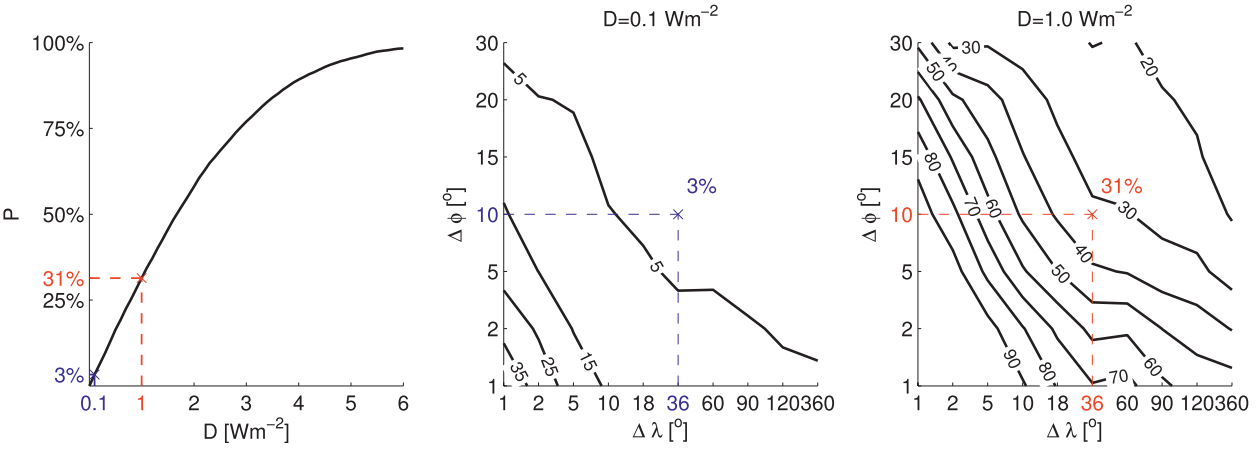

FIG. 4. Percentage of symmetric pairs P. (left) Percentage of symmetric pairs with absolute hemispheric difference in reflected shortwave irradiance smaller than or equal to D for $\Delta\lambda = 36°$ and $\Delta\phi = 10°$. The blue and red crosses mark the percentage of symmetric pairs for $D = 0.1$ and 1.0 W m^{-2}, respectively. (middle) Percentage of symmetric pairs with absolute hemispheric difference in reflected shortwave irradiance smaller than or equal to 0.1 W m^{-2} as a function of $\Delta\lambda$ and $\Delta\phi$. (right) As in (middle), but for $D = 1.0$ W m^{-2}. Time-mean CERES-EBAF edition 2.5A is used.

and on a number of coarser grids. The standard deviation generally decreases with increasing grid spacing because variability and information is lost by averaging to coarser grids. However, there is a first substantial drop in the standard deviation when the meridional grid spacing exceeds 10° latitude. Second, we only take into account every nth latitude circle and compute how much the mean reflected shortwave irradiance of this subsample deviates from the actual global mean. As long as we take into account every 10th latitude circle, the subsample deviates from the global mean by less than 0.5 W m^{-2}. Increasing the subsample's latitudinal spacing to 12°, however, increases the deviation of the subsample from the global mean to 1.4 W m^{-2}. Third, the spectral density of the time-mean, zonal-mean reflected shortwave irradiance shows a pronounced decrease when the wavelength falls below 10° latitude. All three approaches consistently indicate that the time-mean, zonal-mean reflected shortwave irradiance exhibits spatial variability at latitudinal scales of 10° latitude and larger but not at smaller scales. Since $\Delta\phi$ should be set by the smallest contributing scale, we obtain $\Delta\phi = 10°$, which is equivalent to 18 spatial degrees of freedom in the meridional direction.

These estimates of $\Delta\lambda$ and $\Delta\phi$ suggest that the reflected shortwave irradiance has $N = 180$ spatial degrees of freedom and that we should draw random halves on a 36° × 10° grid. Doing so, we find that only 3% of the pairs have a hemispheric difference in reflected shortwave irradiance that is smaller than or equal to the CERES-EBAF measured $D = 0.1$ W m^{-2} (Fig. 4, left). Even when we use a conservative criterion of $D = 1.0$ W m^{-2} that leaves a factor of 10 leeway for measurement uncertainties and brackets the interannual variability of the hemispheric difference as well as the time-mean hemispheric difference in earlier TOA irradiance datasets (cf. section 1), we find that only 31% of the pairs of random halves show hemispheric symmetry. Because the percentage of symmetric pairs is far from 100% even for the conservative choice $D = 1.0$ W m^{-2}, we conclude that the hemispheric symmetry in reflected shortwave irradiance is a nontrivial property of the Earth system. For $D =$ 3 W m^{-2}, the hemispheric symmetry would be trivial, but we would probably not start thinking about hemispheric symmetry if the reflected shortwave irradiance differed by 3 W m^{-2} or more between the hemispheres.

Our test is insensitive to the choice of the EBAF edition as well as to specifics of its construction. To show the latter, we modified our test in three different ways. First, the surface area of the longitude–latitude boxes varies with latitude. Therefore, for most partitionings we need to split one box between the two random halves to make sure that both random halves cover exactly 50% of Earth's surface area. We eliminated the need to split one box by, for each latitude, pooling the Northern and Southern Hemisphere boxes of that latitude and assigning 50% of them to the first random half and the remaining 50% to the second random half. For example, from the $2(360°/\Delta\lambda) = 20$ boxes available at 45°N/S, the first random half could contain 3 boxes from 45°N and 7 from 45°S or all 10 boxes from 45°N and none from 45°S. The second random half then contained 7 boxes from 45°N and 3 from 45°S or no boxes from 45°N and all 10 from 45°S, respectively. Each of the two random halves now embodied half of the boxes with a particular surface area and hence covered exactly 50% of Earth's surface

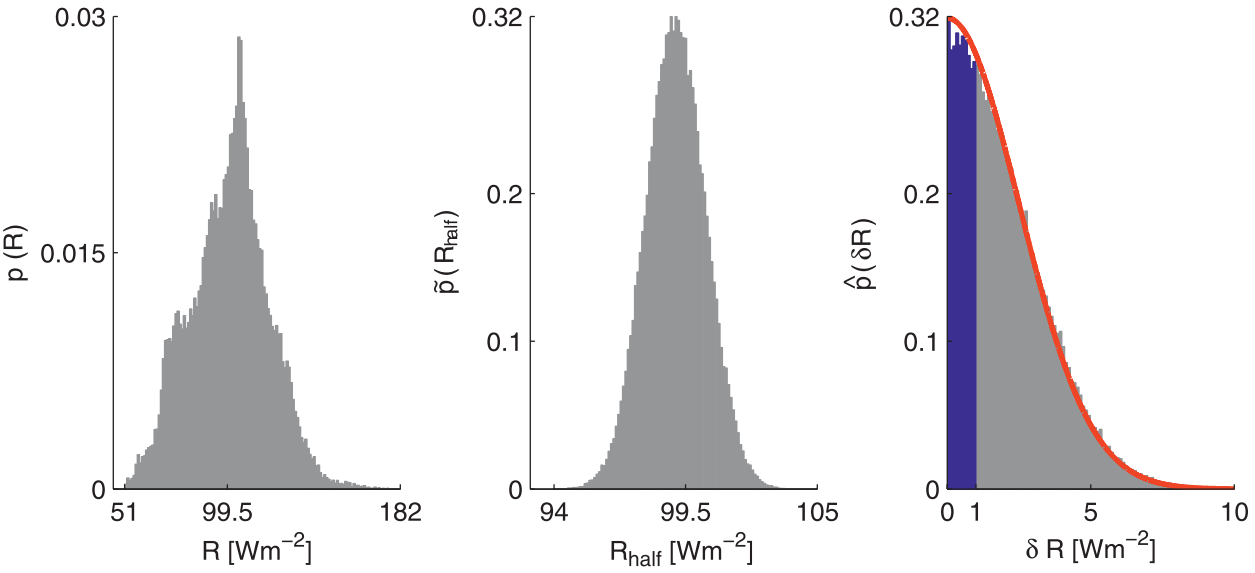

FIG. 5. Estimation of the spatial standard deviation that was required in order for the hemispheric symmetry in reflected shortwave irradiance to be trivial. (left) Area-weighted histogram or population distribution p of time-mean reflected shortwave irradiance R on the native $1° \times 1°$ CERES-EBAF grid. (middle) Sampling distribution $\tilde{p}$ of a random half's reflected shortwave irradiance R_{half} for $\Delta\lambda = 36°$ and $\Delta\phi = 10°$. (right) Distribution $\hat{p}$ of the absolute hemispheric difference in reflected shortwave irradiance of a pair of random halves δR. The red line shows the half-normal distribution that approximates $\hat{p}$ [Eq. (3)]. The blue area measures the percentage of symmetric pairs with $\delta R \leq 1.0$ W m^{-2}. All plots use time-mean reflected shortwave irradiance from CERES-EBAF edition 2.5A.

area, and no box needed to be split. Second, we symmetrized the time-mean, zonal-mean reflected shortwave irradiance with respect to the equator and used the anomalies from this symmetrized field instead of the time-mean reflected shortwave irradiance, thereby taking into account any large-scale meridional structure of the reflected shortwave irradiance. Third, we have combined the two modifications above. None of these three modifications had an appreciable effect on the percentage of symmetric pairs.

If we underestimated the spatial degrees of freedom, we would have arrived at a too low percentage of symmetric pairs P. Having the uncertainty in our estimate of the spatial degrees of freedom in mind, we also draw pairs of random halves on the native $1° \times 1°$ grid of CERES-EBAF as well as various other coarse grids (Fig. 5, right). On a $1° \times 1°$ grid and with a symmetry criterion of $D = 1.0$ W m^{-2}, all pairs of random halves show hemispheric symmetry ($P \simeq 100\%$). This is a result from neglecting spatial autocorrelation and essentially sampling each structure of the reflected shortwave irradiance at least once, so that each of the two random halves of a given pair in fact samples the entire Earth instead of only half of it. More importantly, using $\Delta\lambda = 18°$ (instead of 36°) or $\Delta\phi = 5°$ (instead of 10°), we find that the percentage of symmetric pairs increases only slightly. This indicates that while there is uncertainty in our estimate of the spatial degrees of freedom, this uncertainty does not call into question our result that the observed hemispheric symmetry in reflected shortwave irradiance is a nontrivial property of the Earth system.

3. What spatial standard deviation would be necessary so that the observed hemispheric symmetry in reflected shortwave irradiance could be considered trivial?

The previous section shows that the observed hemispheric symmetry in reflected shortwave irradiance is a nontrivial property of the Earth system. Assuming that the spatial degrees of freedom are given, one can interpret this result as being caused by a large spatial standard deviation of the observed reflected shortwave irradiance. In this section, we derive an equation that allows us to calculate the spatial standard deviation necessary so that the hemispheric symmetry in reflected shortwave irradiance could be considered trivial. We will find that the spatial standard deviation of the reflected shortwave irradiance would need to be 4 times smaller than what is observed.

We start with the central limit theorem. The central limit theorem states that, for a large enough sample size, the distribution of the sample mean approaches a normal distribution that is centered at the mean of the population distribution. In our case, the population distribution

is the area-weighted histogram of CERES-EBAF time-mean reflected shortwave irradiance with global-mean $\overline{R} = 99.5\ \mathrm{W\ m^{-2}}$ (Fig. 5, left). By drawing random halves and calculating their reflected shortwave irradiance R_{half}, we generate the sampling distribution, denoted by $\tilde{p}(R_{\mathrm{half}})$. Here, $\tilde{p}(R_{\mathrm{half}})$ is the probability that the reflected shortwave irradiance of a random half is R_{half}. It follows from the central limit theorem that $\tilde{p}(R_{\mathrm{half}})$ is nearly normal and centered at $\overline{R}$ (Fig. 3, middle),

$$\tilde{p}(R_{\mathrm{half}}) = \frac{1}{\sqrt{2\pi\tilde{\sigma}^2}} \exp\left[-\frac{(R_{\mathrm{half}} - \overline{R})^2}{2\tilde{\sigma}^2}\right], \qquad (1)$$

where $\tilde{\sigma}$ is the standard deviation of $\tilde{p}(R_{\mathrm{half}})$.

For a given $(\Delta\lambda, \Delta\phi)$, Earth consists of $N = (360°/\Delta\lambda)(180°/\Delta\phi)$ latitude boxes of which about 50% are needed to construct a random half. The central limit theorem tells us that $\tilde{\sigma}$ is therefore given by (Freund 1974, p. 230)

$$\tilde{\sigma}(\Delta\lambda, \Delta\phi) \simeq \frac{\sigma}{\sqrt{N/2}} \sqrt{\frac{N/2}{N-1}} \simeq \frac{\sigma}{\sqrt{N}}, \qquad (2)$$

where $\tilde{\sigma}$ depends on $(\Delta\lambda, \Delta\phi)$ through both $N(\Delta\lambda, \Delta\phi)$ and the spatial standard deviation of the time-mean CERES-EBAF reflected shortwave irradiance on a $(\Delta\lambda, \Delta\phi)$ grid, $\sigma(\Delta\lambda, \Delta\phi)$.

For a pair with one random half deviating from the global-mean reflected shortwave irradiance by $R - \overline{R}$, the other random half deviates from the global-mean reflected shortwave irradiance by $-(R - \overline{R})$. The pair hence has an absolute hemispheric asymmetry of $\delta R = 2|(R - \overline{R})|$. From Eqs. (1) and (2), it follows that the sampling distribution of the pairs' absolute asymmetry is nearly half normal (Fig. 5, right),

$$\hat{p}(\delta R; \Delta\lambda, \Delta\phi) = \frac{1}{\sqrt{2\pi}\tilde{\sigma}} \exp\left(-\frac{\delta R^2}{8\tilde{\sigma}^2}\right) \simeq \sqrt{\frac{N}{2\pi}} \frac{1}{\sigma} \exp\left(-\frac{N\delta R^2}{8\sigma^2}\right). \qquad (3)$$

With this, the percentage of symmetric pairs as a function of D is given by

$$P(D; \Delta\lambda, \Delta\phi) = \int_0^D \hat{p}(\delta R; \Delta\lambda, \Delta\phi)\, d\delta R \simeq \sqrt{\frac{N}{2\pi}} \frac{1}{\sigma} \int_0^D \exp\left(-\frac{N\delta R^2}{8\sigma^2}\right) d\delta R \simeq \mathrm{erf}\left(\sqrt{\frac{N}{8}} \frac{D}{\sigma}\right). \qquad (4)$$

Here, erf is the error function. If we finally approximate $\sigma(\Delta\lambda, \Delta\phi) \simeq \sigma(1°, 1°)$ in Eq. (4), we obtain

$$P(D; \Delta\lambda, \Delta\phi) \simeq \mathrm{erf}\left[\sqrt{\frac{N}{8}} \frac{D}{\sigma(1°, 1°)}\right]. \qquad (5)$$

We can use Eq. (5) to calculate how small the spatial standard deviation would need to be in order for the hemispheric symmetry to be trivial. With $N = 180$ from $(\Delta\lambda, \Delta\phi) = (36°, 10°)$ and $D = 1.0\ \mathrm{W\ m^{-2}}$, 90% of the pairs would be classified symmetric when $\sigma(1°, 1°) \leq 4\ \mathrm{W\ m^{-2}}$. Therefore, for the hemispheric symmetry in reflected shortwave irradiance to be trivial, the spatial standard deviation of the reflected shortwave irradiance would need to be a factor of 4 smaller than in the observations ($18.7\ \mathrm{W\ m^{-2}}$).

4. Do CMIP3 climate models reproduce the observed hemispheric symmetry in reflected shortwave irradiance?

In this section, we explore the hemispheric difference in reflected shortwave irradiance in climate model simulations. Exploring climate model simulations offers an additional way to test whether the observed hemispheric symmetry is trivial. If the observed hemispheric symmetry was trivial, then climate models should generate small hemispheric differences in reflected shortwave irradiance, at least if we assume that climate models well represent the statistical properties of the observed reflected shortwave irradiance. This assumption appears reasonable for two reasons. First, the spatial degrees of freedom of the reflected shortwave irradiance should largely depend on the spatial degrees of freedom in the distribution of clouds. The latter are tied to the large-scale atmospheric dynamics, which models represent in a satisfactory manner. Second, the spatial standard deviations of the models' reflected shortwave irradiance are generally close to the observed value (see below).

We use Atmospheric Model Intercomparison Project (AMIP) simulations driven by observed sea surface temperatures from 1980 to 1999, for which we verified that the Northern and Southern Hemispheres receive the same amount of incident shortwave irradiance in all models (not shown). These simulations are part of the World Climate Research Programme (WCRP) Coupled Model Intercomparison Project phase 3 (CMIP3) multimodel dataset (Meehl et al. 2007).

In agreement with CERES-EBAF, all models show larger clear-sky reflected shortwave irradiance in the Northern Hemisphere (Fig. 6, left). Consistent between models, the magnitude of the hemispheric difference is smaller in the all sky than the clear sky. This is plausible

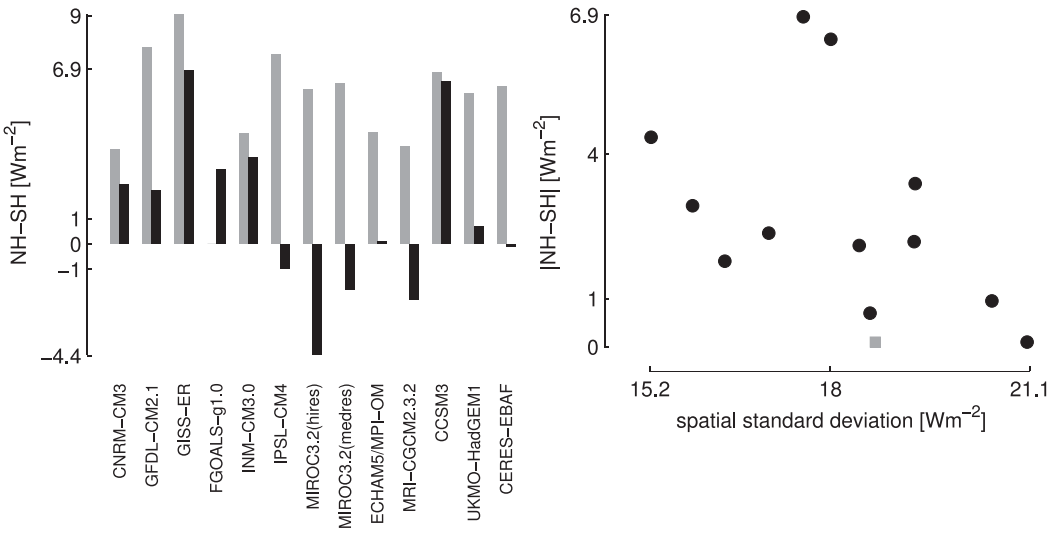

FIG. 6. (left) Hemispheric difference (Northern Hemisphere minus Southern Hemisphere) in reflected shortwave irradiance of CMIP3 AMIP climate simulations with prescribed observed sea surface temperatures. Gray bars show clear-sky differences, and black bars show all-sky differences. For the Flexible Global Ocean–Atmosphere–Land System Model, gridpoint version 1.0 (FGOALS-g.1.0), clear-sky reflected shortwave irradiance is not available in the CMIP3 archive. CERES-EBAF Ed2.5A is included for comparison with observations. (Right) For the same simulations, absolute hemispheric difference in reflected shortwave irradiance in dependence of the spatial standard deviation of reflected shortwave irradiance. The gray square shows the CERES-EBAF Ed2.5A values.

from the fact that the shortwave radiative effect of clouds tends to be larger in regions with low clear-sky (and hence surface) albedo. For example, the same cloud has less shortwave radiative effect over ice-covered regions than over dark ocean areas. Indeed, if cloud albedo and cloud fraction were spatially uniform, clouds would attenuate a clear-sky hemispheric difference by about 65%, where the attenuating magnitude is given by the cloud fraction in percent. To see this, we write the all-sky reflected shortwave irradiance as

$$R = \alpha_{\text{cloud}} f_{\text{cloud}} S + \alpha_{\text{clear}}(1 - f_{\text{cloud}})S, \qquad (6)$$

where α_{cloud} is cloud albedo, f is cloud fraction, α_{clear} is clear-sky planetary albedo, and S is incident shortwave irradiance. With clear-sky reflected shortwave irradiance given by $R_{\text{clear}} = \alpha_{\text{clear}} S$, Eq. (6) becomes

$$R = \alpha_{\text{cloud}} f_{\text{cloud}} S + R_{\text{clear}}(1 - f_{\text{cloud}}). \qquad (7)$$

Assuming spatially uniform cloud albedo and cloud cover, the hemispheric difference in reflected shortwave irradiance is

$$R^{\text{NH}} - R^{\text{SH}} = (1 - f_{\text{cloud}})(R^{\text{NH}}_{\text{clear}} - R^{\text{SH}}_{\text{clear}}), \qquad (8)$$

where NH and SH denote Northern and Southern Hemisphere values, respectively. With $f_{\text{cloud}} = 0.65$ being a typical value for global-mean cloud cover in CMIP3 models (Bender 2011), introducing spatially uniform clouds attenuates the clear-sky hemispheric difference by 65%. However, the shading effect cannot explain the opposite signs of the clear-sky and all-sky hemispheric differences found in some of the models. Moreover, the shading effect is unable to explain the observed hemispheric symmetry.

Most AMIP simulations exhibit considerable hemispheric difference in reflected shortwave irradiance. Out of 12 models, 9 show an all-sky hemispheric difference of more than 1 W m^{-2}; only one model captures the observed hemispheric symmetry (Fig. 6, left). Notably, the model spread in the all-sky hemispheric difference is twice as large as the spread in the clear-sky hemispheric difference, and models disagree in the sign of the all-sky but not the clear-sky hemispheric difference. This illustrates the models' difficulties in simulating the regional distribution of clouds, leading to large regional biases in the modeled shortwave irradiance (Stevens and Schwartz 2012).

The climate model ensemble shows no evidence for a positive correlation between the magnitude of the hemispheric difference and the spatial standard deviation of the modeled reflected shortwave irradiance (Fig. 6, right). If anything, the correlation is negative. Hence, climate models with smaller spatial standard deviation of reflected shortwave irradiance do not tend to simulate

a smaller hemispheric difference. Both the lack of such a positive correlation and the fact that climate models generally do not capture the observed hemispheric symmetry provide further evidence that the observed hemispheric symmetry in reflected shortwave irradiance is nontrivial.

5. Conclusions

We study CERES-EBAF data from 2000 to 2010 and find that the Northern and Southern Hemispheres over the last decade have reflected the same amount of shortwave irradiance. This hemispheric symmetry in reflected shortwave irradiance translates to a hemispheric symmetry in planetary albedo. Because earlier TOA irradiance datasets also show a small hemispheric difference in reflected shortwave irradiance, the hemispheric symmetry in reflected shortwave irradiance appears to be a robust feature of the observed climate system.

By partitioning Earth into pairs of random halves, we show that the hemispheric symmetry in reflected shortwave irradiance is a nontrivial property of the Earth system. Only 30% of the pairs exhibit hemispheric symmetry within 1%, or 1 W m^{-2}. This test requires us to estimate the spatial degrees of freedom of the CERES-EBAF reflected shortwave irradiance. To our knowledge, there is no unique way to estimate these, and other techniques than the ones presented here might yield different estimates. However, as we show by drawing random halves on various grids, the uncertainty in the spatial degrees of freedom does not substantially affect the percentage of symmetric pairs. Moreover, our criterion to distinguish symmetric from asymmetric pairs is rather conservative as it is 10 times larger than the hemispheric difference observed by CERES-EBAF.

We demonstrate that, because the shortwave radiative effect of clouds is larger in regions with low clear-sky albedo, one expects the all-sky hemispheric difference in reflected shortwave irradiance to be smaller than the clear-sky hemispheric difference. However, this shading effect of clouds is unable to explain the observed hemispheric symmetry in reflected shortwave irradiance. Moreover, we show that climate models generally do not reproduce the observed hemispheric symmetry in reflected shortwave irradiance. This supports our result that the observed hemispheric symmetry is nontrivial.

Our test cannot rule out that the observed hemispheric symmetry is accidental. Nevertheless, our results motivate to research into mechanisms that minimize the hemispheric difference in reflected shortwave irradiance. We believe that any such mechanism must involve clouds because clouds are the largest contributor to planetary albedo (e.g., Ramanathan et al. 1989; Donohoe and Battisti 2011) and are required to level the observed 6 W m^{-2} hemispheric difference in clear-sky reflected shortwave irradiance caused by hemispheric asymmetries in landmasses and aerosol loading. We expect that a possible compensating mechanism involves the location of the ITCZ and of tropical cloud cover, which should be important for the hemispheric difference in reflected shortwave irradiance simply because incident shortwave irradiance is largest in the tropics. Climate models (Chiang and Bitz 2005) as well as proxy data from past climates (e.g., Lea et al. 2003; Pahnke et al. 2007; Holbourn et al. 2010) suggest that increasing high-latitude ice cover in one hemisphere leads to a shift of the ITCZ into the other hemisphere. The resulting change in the tropical cloud cover would dampen the hemispheric difference in reflected shortwave irradiance that is generated by the hemispheric difference in ice cover. Such a compensating ITCZ shift is also suggested by the simulations of Kang et al. (2008), which moreover demonstrated that the location of the ITCZ is influenced by the ocean's energy transport. This suggests that compensating mechanisms involve the ocean's circulation. Whether such compensating mechanisms indeed exist needs to be investigated by future studies.

Acknowledgments. We thank the two anonymous reviewers for their comments and the editor Dr. Brian Soden for help with evaluating the manuscript. We are grateful to Lorenzo Tomassini for a careful internal review at MPI-M, and we enjoyed discussions with Ian Eisenman on an earlier version of this manuscript. This research was supported by the Max Planck Society for the Advancement of Science. The CERES-EBAF data have been obtained online (edition 1A at http://eosweb.larc.nasa.gov/PRODOCS/ceres/level4_ebaf_table.html; editions 2.5A and 2.6r at http://ceres.larc.nasa.gov/order_data.php). We acknowledge the modeling groups, the Program for Climate Model Diagnosis and Intercomparison (PCMDI) and the WCRP Working Group on Coupled Modelling (WGCM), for their roles in making available the WCRP CMIP3 multimodel dataset. Support of this dataset and this research is provided by the U.S. Department of Energy Office of Science.

REFERENCES

Bender, F., 2011: Planetary albedo in strongly forced climate, as simulated by the CMIP3 models. *Theor. Appl. Climatol.,* **105,** 529–535, doi:10.1007/s00704-011-0411-2.

Chiang, J., and C. Bitz, 2005: Influence of high latitude ice cover on the marine intertropical convergence zone. *Climate Dyn.,* **25,** 477–496, doi:10.1007/s00382-005-0040-5.

Donohoe, A., and D. S. Battisti, 2011: Atmospheric and surface contributions to planetary albedo. *J. Climate,* **24,** 4402–4418.

Fortin, M., and M. Dale, 2005: *Spatial Analysis: A Guide for Ecologists.* Cambridge University Press, 380 pp.

Freund, J. E., 1974: *Modern Elementary Statistics.* 4th ed. Prentice-Hall International, 532 pp.

Geogdzhayev, I. V., M. I. Mishchenko, E. I. Terez, G. A. Terez, and G. K. Gushchin, 2005: Regional advanced very high resolution radiometer–derived climatology of aerosol optical thickness and size. *J. Geophys. Res.,* **110,** D23205, doi:10.1029/2005JD006170.

Hatzianastassiou, N., A. Fotiadi, C. Matsoukas, K. Pavlakis, E. Drakakis, D. Hatzidimitriou, and I. Vardavas, 2004a: Long-term global distribution of earth's shortwave radiation budget at the top of atmosphere. *Atmos. Chem. Phys.,* **4,** 1217–1235, doi:10.5194/acp-4-1217-2004.

——, C. Matsoukas, D. Hatzidimitriou, C. Pavlakis, M. Drakakis, and I. Vardavas, 2004b: Ten year radiation budget of the earth: 1984–93. *Int. J. Climatol.,* **24,** 1785–1802, doi:10.1002/joc.1110.

Holbourn, A., W. Kuhnt, M. Regenberg, M. Schulz, A. Mix, and N. Andersen, 2010: Does Antarctic glaciation force migration of the tropical rain belt? *Geology,* **38,** 783–786, doi:10.1130/G31043.1.

Kang, S. M., I. M. Held, D. M. W. Frierson, and M. Zhao, 2008: The response of the ITCZ to extratropical thermal forcing: Idealized slab-ocean experiments with a GCM. *J. Climate,* **21,** 3521–3532.

Kato, S., 2009: Interannual variability of the global radiation budget. *J. Climate,* **22,** 4893–4907.

Kishcha, P., B. Starobinets, O. Kalashnikova, C. N. Long, and P. Alpert, 2009: Variations of meridional aerosol distribution and solar dimming. *J. Geophys. Res.,* **114,** D00D14, doi:10.1029/2008JD010975.

Lea, D. W., D. K. Pak, L. C. Peterson, and K. A. Hughen, 2003: Synchroneity of tropical and high-latitude Atlantic temperatures over the last glacial termination. *Science,* **301,** 1361–1364.

Loeb, N. G., B. A. Wielicki, D. R. Doelling, G. L. Smith, D. F. Keyes, S. Kato, N. Manalo-Smith, and T. Wong, 2009: Toward optimal closure of the earth's top-of-atmosphere radiation budget. *J. Climate,* **22,** 748–766.

Meehl, G. A., C. Covey, K. E. Taylor, T. Delworth, R. J. Stouffer, M. Latif, B. McAvaney, and J. F. B. Mitchell, 2007: The WCRP CMIP3 multimodel dataset: A new era in climate change research. *Bull. Amer. Meteor. Soc.,* **88,** 1383–1394.

Pahnke, K., J. P. Sachs, L. Keigwin, A. Timmermann, and S.-P. Xie, 2007: Eastern tropical Pacific hydrologic changes during the past 27,000 years from D/H ratios in alkenones. *Paleoceanography,* **22,** PA4214, doi:10.1029/2007PA001468.

Pierrehumbert, R. T., 2010: *Principles of Planetary Climate.* Cambridge University Press, 680 pp.

Ramanathan, V., 1987: The role of Earth radiation budget studies in climate and general circulation research. *J. Geophys. Res.,* **92** (D4), 4075–4095.

——, R. D. Cess, E. F. Harrison, P. Minnis, B. R. Barkstrom, E. Ahmad, and D. Hartmann, 1989: Cloud-radiative forcing and climate: Results from the Earth Radiation Budget Experiment. *Science,* **243,** 57–63.

Stevens, B., and S. E. Schwartz, 2012: Observing and modeling Earth's energy flows. *Surv. Geophys.,* **33,** 779–816.

Vonder Haar, T. H., and V. E. Suomi, 1971: Measurements of the earth's radiation budget from satellites during a five-year period. Part I: Extended time and space means. *J. Atmos. Sci.,* **28,** 305–314.

Wielicki, B. A., B. R. Barkstrom, E. F. Harrison, R. B. Lee, G. Louis Smith, and J. E. Cooper, 1996: Clouds and the Earth's Radiant Energy System (CERES): An Earth Observing System experiment. *Bull. Amer. Meteor. Soc.,* **77,** 853–868.

Zhang, Y.-C., and W. B. Rossow, 1997: Estimating meridional energy transports by the atmospheric and oceanic general circulations using boundary fluxes. *J. Climate,* **10,** 2358–2373.